Acta Poloniae Pharmaceutica – Drug Research, Vol. 72 No. 1 pp. 179–192, 2015 ISSN 0001-6837
Polish Pharmaceutical Society

AMORPHOUS SOLID DISPERSION STUDIES OF CAMPTOTHECIN–CYCLODEXTRIN INCLUSION COMPLEXES IN PEG 6000

SOFIANE FATMI[1, 2, 3], LAMINE BOURNINE[4], MOKRANE IGUER-OUADA[3], MALIKA LAHIANI-SKIBA[1], FATIHA BOUCHAL[2] and MOHAMED SKIBA[1]*

[1] Technology Pharmaceutical and Biopharmaceutics Laboratory, UFR Medicine and Pharmacy, Rouen University, 22 Blvd. Gambetta, 76183, Rouen, France
[2] Technology Pharmaceutical Laboratory, Department of Engineering Processes,
[3] Marine Ecosystems and Aquaculture Laboratory, [4] Plant Biotechnology and Ethnobotany Laboratory, Faculty of Natural Sciences and Life, Abderrahmane-Mira University, Targua Ouzemmour road, 06000 Bejaia, Algeria

Abstract: The present work focused on the solubility enhancement of the poorly water-soluble anti-cancer agent camptothecin which, in its natural state, presents poor solubility inducing lack of activity with a marked toxicity. A new approach is adopted by using a ternary system including camptothecin (CPT) and cyclodextrins (CDs) dispersed in polyethylene glycol (PEG) 6000. Camptothecin solubility variations in the presence of α-CD, β-CD, γ-CD, hydroxypropyl-α-CD (HPα-CD), hydroxypropyl-β-CD (HPβ-CD), permethyl-β-CD (PMβ-CD) and sulfobutyl ether-β-CD (SBEβ-CD), were evaluated by Higuchi solubility experiments. In the second part, the most efficient camptothecin/β-CDs binary systems, mainly HPβ-CD and PMβ-CD, were dispersed in PEG 6000. In addition to a drug release and modeling evaluation, the CPT interactions with CDs and PEG 6000 to prepared the amorphous solid dispersion in the binary and ternary systems were investigated by Fourier transformed infrared spectroscopy (FT-IR), differential scanning calorimetry (DSC), thermogravimetric analyses (TGA) and X-ray powder diffraction (XRPD). The results showed that HPβ-CD and PMβ-CD were the most efficient for camptothecin solubilization with highest apparent equilibrium constants. Dissolution studies showed that percentage of CPT alone after two hour in 0.1 M HCl medium, did not exceed 16%, whereas under the same conditions, CPT/PMβ-CD complex reached 76%. When dispersing the binary systems CPT/β-CDs in PEG 6000, the velocity and the percentage of CPT release were considerably improved whatever the CD used, reaching the same value of 85%. The binary and ternary systems characterization demonstrated that CPT inclused into the CDs cavity, replacing the water molecules. Furthermore, a drug transition from crystalline to amorphous form was obtained when solid dispersion is realized. The present work demonstrated that ternary complexes are promising systems for CPT encapsulation, and offer opportunities to use non toxic and commonly solubilizing carriers: βCD and PEG 6000 to improve bioavailability.

Keywords: camptothecin, cyclodextrins, kinetic model, PEG 6000, amorphous solid dispersion characterization, ternary complex

Camptothecin (CPT, Fig. 1) is an anti-cancer agent belonging to the family of the alkaloids, it is present in wood, bark and fruit of the Asian tree *Camptotheca acuminata* (1, 2). Camptothecin is known as DNA topoisomerase I inhibitor (3, 4) presenting a powerful anti-cancer activity against a wide spectrum of human malignancies, such as lung, prostate, breast, colon, stomach and ovarian carcinomas (5). However, the full therapeutic potential of CPT is limited in relation to its poor solubility (6) inducing lack of activity, with a marked toxicity (7). This limited activity is mainly in relation to the pH dependent behavior of the lactone ring (Fig. 1) (7, 8).

Several approaches are proposed to improve CPT or analogs solubility; especially the use of various polymers such as: polyethylene glycol (PEG) (5, 9–11), poly(lactide-Co-glycolide), polycaprolactone (12), o-carboxymethylchitosan (13) and cyclodextrins (CDs) (14–16).

Cyclodextrins are cyclic oligosaccharides composed of glucose units linked to each other by α (1→4) glycosidic bond. Three natural types of cyclodextrins are reported: α-cyclodextrin (α-CD),

* Corresponding author: e-mail: mohamed.skiba@univ-rouen.fr

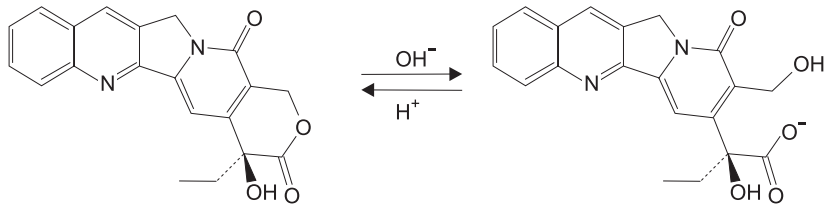

Figure 1. CPT structure (active and inactive form) (9)

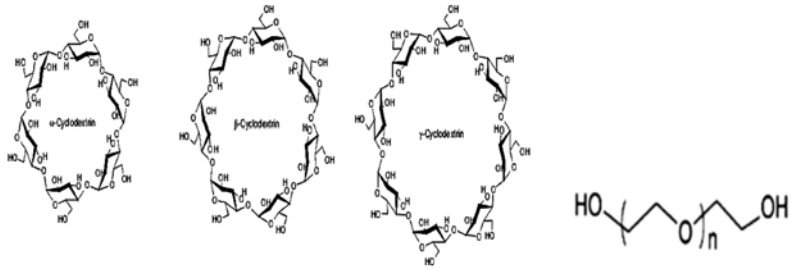

Figure 2. Molecular structure of natural cyclodextrins (24) and polyethylene glycol (25)

β-cyclodextrin (β-CD) and γ-cyclodextrin (γ-CD) composed of 6, 7 and 8 units of glucopyranoses (Fig. 2), respectively (17, 18). They result from the enzymatic degradation of the starch by cyclodextrins glucosyl transferases (CGTases) (18). The glucose units are bonded together to form a truncated cone shaped molecule with a broadest end containing secondary and tertiary hydroxyls, and a narrowest end containing primary hydroxyls (19). As a consequence, the inner cavity of cyclodextrins is hydrophobic and the exterior hydrophilic (20). This fact is used to increase molecules aqueous solubility by inclusion complexes (21).

In the present work, solubility of camptothecin in the presence of various CDs: α-CD, β-CD, γ-CD, hydroxypropyl-α-CD (HPα-CD), hydroxypropyl-γ-CD (HPγ-CD), hydroxypropyl-β-CD (HPβ-CD), permethyl-β-CD (PMβ-CD) and sulfobutyl ether-β-CD (SBEβ-CD) was investigated and the equilibrium constants (Kc) were determined. Inclusion complexes were prepared and dissolution profiles were studied.

A new approach was also investigated to enhance CPT solubility by a ternary system: complexes CPT/CD dispersed in PEG (Fig. 2). The later, is a water-soluble, nontoxic, non-antigenic, biocompatible polymer that has been approved by the Food and Drug Administration for human intravenous, oral, and dermal applications (22), its most common form is a linear or branched polyether ended with hydroxyl groups (23). In order to investigate the effect of PEG on both camptothecin and its corresponding inclusion complexes, dissolution profiles were realized. Finally, the nature of interaction in binary and ternary systems, were studied using different methods: Fourier transformed infrared spectroscopy (FT-IR), differential scanning calorimetry (DSC), thermogravimetric analyses (TGA) and X-ray powder diffraction (XRPD).

MATERIALS AND METHODS

Materials

Drug

Camptothecin (M.w. 348.11 g/mol) was purchased from Shenzhen Boda Natural Product laboratory (P. R. China).

Cyclodextrins

β-CD was obtained from Roquette Frères (France) (1135 g/mol), α-CD (972 g/mol), γ-CD (1297 g/mol), hydroxypropyl-β-CD (HPβ-CD, 1488 g/mol), hydroxypropyl-α-CD (HPα-CD, 1285 g/mol) and hydroxypropyl-γ-CD (HPγ-CD, 1713

g/mol) were provided by Wacker (Germany). Permethylated β-CD (PMβ-CD, 1330 g/mol) was received from Orsan (France). Sulfobutyl ether β-CD, SBE-CD (2163 g/mol) was purchased from Cydex, Inc. (USA).

Polyethylene glycol

PEG 4000 and 6000 were obtained from BASF (Germany).

All reagents were of analytical grade.

Methods

HPLC analyses

The analysis of lactone and carboxylate forms of CPT in solubility study, were performed using HPLC system which consisted of Jasco PU-980 pomp, Jasco AS-950 auto injector and Merck multichannel photo Detector L 3000, equipped with C-18 analytical column. The mobile phase consisted of a mixture of a borate buffer and acetonitrile (65 : 35, v/v). Standard solution was prepared by dissolving CPT in a mixture of acetone / DMSO (95 : 5, v/v).

Solubility experiments and apparent equilibrium constant determination

The solubility measurement was carried out according to the method of Higuchi and Connors reported by Brewster and Loftsson (26). Excess of CPT was suspended in 5 mL pH 2.0 phosphate buffer solution (PBS pH 2) containing increasing concentrations of CDs : γ-CD (0–180 M), β-CD (0–16 mM), a-CD (0–150 mM), PMβ-CD (0–300 mM), SBEβ-CD (0–90 mM), HPγ-CD (0–350 M), HPβ-CD (0–467 mM) and HPa-CD (0–300 mM), all solutions were shaken at 37°C under a constant agitation rate. Aliquots were withdrawn at the equilibrium after one week. The aliquots were filtered through 0.45 μm membrane and quantified by HPLC. Each experiment was carried out in duplicate. The apparent binding constants were calculated from the straight line portion of the phase solubility diagram according to Higuchi-Connors, given in equation (1):

$$Kc = \text{slope} / So\ (1\text{-slope}) \qquad \text{(Equation 1)}$$

where So = drug solubility without CDs.

Preparation of binary systems

Solid inclusion complexes prepared by solvent evaporation method

Cyclodextrins and CPT in a 1 : 1 molar ratio were dissolved in 50 mL of ethanol, the mixture was left under agitation for 1 h protected from light. After drying at 45°C during 1 h, the powder was preserved in a dessicator.

Solid dispersion (SD) CPT/ PEGs

Mixtures of CPT/ PEG 6000 or PEG 4000 at 5/95, 10/90, 15/85 and 30/70% (w/w) were dissolved in ethanol by agitation. After drying at 45°C during 1 h, the powder was preserved in a dessicator.

Preparation of ternary systems

Solid dispersion CPT complexes / PEG 6000

Nine parts of polyethylene glycol 6000 and one part of CPT in its complexes form were dissolved in ethanol by agitation. After drying at 45°C during 1 h, the powder was preserved in a dessicator.

Physical mixtures

Nine part of polyethylene glycol 6000 and one part of CPT in complexes form were mixed in a mortar until obtaining an apparent homogeneous powder. The latter was preserved in a dessicator.

Characterization of inclusion complexes and solid dispersions

Fourier transformed infrared spectroscopy (FT-IR)

The FT-IR spectra were taken from dried samples. An FT-IR machine from PerkinElmer equipped with an ATR was used in the frequency between 4000 cm^{-1} and 700 cm^{-1}.

Differential scanning calorimetry (DSC)

Thermal analysis was performed using a PerkinElmer differential scanning calorimeter (DSC-4), which was equipped with a compensated power system. All samples were weighed at around 5 mg and heated at a scanning rate of 10°C/min to a temperature level between 30 and 350°C under a nitrogen gas flow. Aluminum pans and lids were used for all samples.

Thermogravimetric analysis (TGA)

TGA was carried out using thermal analyzer (PerkinElmer, USA) with attached TG unit. The sample was heated under normal atmosphere at a rate of 10°C/min, and the loss of weight was recorded in temperature range 30 to 750°C for the pure drug and from 30 to 650°C for other samples.

X-ray powder diffraction (XRPD)

X-ray diffractograms of CPT, carriers, binary and ternary systems were recorded using an X-ray diffractometer (X'Pert Propan analytical, Netherlands) using RTMS detector, generated at 40 kV and 30 mA and scanning rate of 2°/min over a 2θ range of 0°–70°.

Dissolution studies

Dissolution profiles of free CPT, inclusion complexes or SDs were evaluated. Briefly, 10 mg of free CPT or its equivalent of complexes or SDs were added to 900 mL of hydrochloric acid (0.1 M) at 37 ± 0.5°C, the rotation speed paddle was fixed at 75 rpm. The amount of dissolved CPT was evaluated on Beckman DU 640 B spectrophotometer at 286 nm. Each analysis was repeated in triplicate.

Drug release kinetics

In order to establish the mathematical model of CPT release from different preparations, the experimental data were fitted to commonly kinetic models (like zero order, first order, Higuchi, and Korsmeyer-Peppas) reported by Tapan et al. (27), where:

Zero-order model: $F = K_0 t$, where F represents the fraction of drug released in time t and K_0 is the apparent release rate constant or zero-order release constant.

First-order model: $\ln (1–F) = K1^{st} t$, where F represents the fraction of drug released in time t and $K1^{st}$ is the first-order release constant.

Higuchi model: $F = K_H t^{1/2}$, where F represents the fraction of drug released in time t and K_H is the Higuchi dissolution constant.

Korsmeyer-Peppas model: $F = K_P t^n$, where F represents the fraction of drug released in time t, K_P is the rate constant and n is the diffusional exponent, it indicates the drug release mechanism (28–30).

RESULTS AND DISCUSSION

Solubility experiment

The solubility of CPT according to different CDs concentrations is shown in Figures 3–5. The CPT apparent solubility increased with CDs concentration. When using natural or modified β-CDs, CPT solubility increased linearly, it exhibits typical *AL* curves corresponding to equivalent molar ratio between CD and CPT as reported by Kang et al. (15) and Foulon et al. (31). The apparent equilibrium constant (Kc), is calculated using an equation proposed by Higuchi and Conners:

$$Kc = So / \text{intercept } (1\text{-slope}) \quad \text{(Equation 2)}$$

where So = drug solubility without CDs.

The modified and natural α- and γ-CDs showed *AP* curves. As described by Brewster (26), it is corresponding to CPT/CDs 1 : 2, 1 : 3 molar ratios. The Kc in this case is calculated using the linear portion of the curves. The maximal apparent CPT solubility and equilibrium constant are reported in Table 1.

Among the natural CDs, αCD induced the greatest increase in CPT solubility with approximately sixteen folds compared to CPT alone. βCD and γCD, in contrast, increased two- and twelve folds CPT solubility, at their water solubility limit, respectively. These results suggest that αCD is the most effective solubilizing agent for CPT. This is in relation to its higher intrinsic solubility compared to βCD, with a more adequate size cavity compared to γCD. However, when working at low CD concentrations, 1.5% (w/v) for βCD and 2.5% (w/v) for αCD and γCD, respectively, Kang et al. (15) found that βCD is more effective in solubilizing CPT. According to Brewster (26), the solubility study should be realized at CDs water solubility limit.

Among the three modified HP-CDs (HPα, HPβ and HPγ), HP-β-CD solubilized CPT to the greatest extent. Around water solubility limit of each HP-CDs (HPα, HPβ and HPγ), camptothecin solubility was increased by factor of 47, 70 and 43, respectively, when compared to CPT alone. It has been shown previously that HP cyclodextrins

Table 1. Solubility and equilibrium constants (Kc) for camptothecin complexes calculated from the slope of the best-fit line of the phase solubility.

CDs	CPT max (10^{-3} mM)	So mM	slope	Smax/So	Kc (M^{-1})
βCD 16 mM	1.84E+01	8.15E–03	1.19E–03	2.26E+00	1.46E+02
αCD 150 mM	1.32E+02	8.15E–03	4.63E–04	1.62E+01	5.69E+01
γCD 180 mM	1.03E+02	8.15E–03	5.07E–04	1.27E+01	6.22E+01
HPβCD 300 mM	5.71E+02	8.15E–03	1.97E–03	7.01E+01	2.43E+02
HPαCD 420.6 mM	3.80E+02	8.15E–03	1.04E–03	4.66E+01	1.28E+02
HPγCD 350 mM	3.50E+02	8.15E–03	5.58E–04	4.29E+01	6.85E+01
SBEβCD 90 mM	2.32E+02	8.15E–03	2.30E–03	2.85E+01	2.83E+02
PMβ-CD 300 mM	2.13E+03	8.15E–03	4.70E–03	2.61E+02	5.79E+02

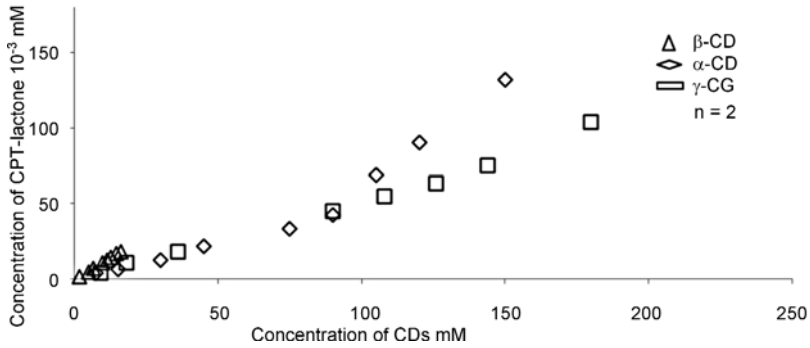

Figure 3. Solubility diagrams of camptothecin in the presence of natural CDs

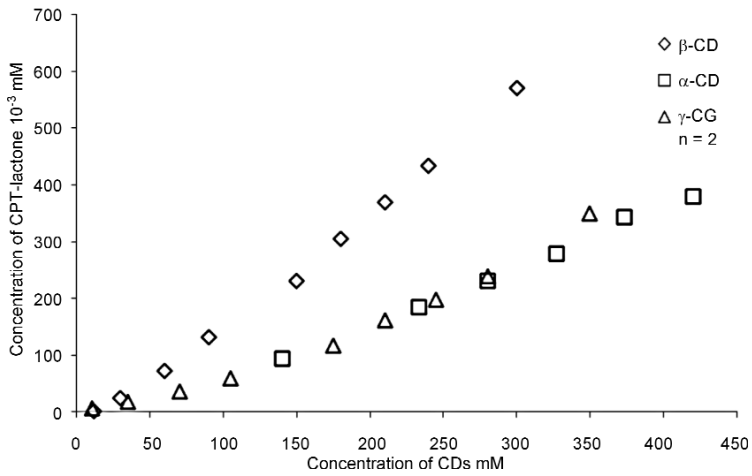

Figure 4. Solubility diagrams of camptothecin in the presence of HPCDs

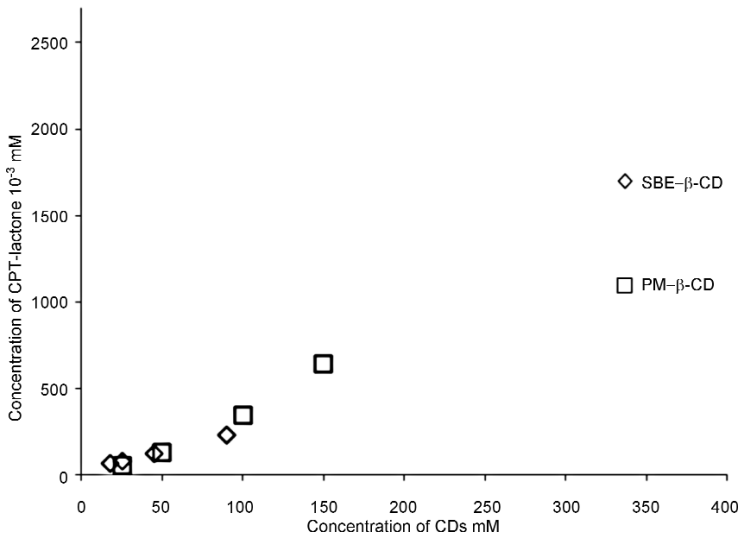

Figure 5. Solubility diagrams of camptothecin in the presence of SBE-β-CD and PM-β-CD

improved solubility by the presence of hydroxypropyl groups (19). These results suggest also that β-CD cavity size is more adequate to CPT.

At 90 mM of SBE-β-CD, camptothecin solubility was increased by factor of 28 compared to the value obtained with CPT alone.

Among CDs tested in the present work, the most efficient is PM-β-CD in improving camptothecin solubility which was increased by 261 folds when compared to CPT alone. This could be attributed to the presence of methyl groups, which not only disrupt hydrogen bonding, but also enlarge the whole cavity (14).

The equilibrium constants (Table 1) were in agreement with the values described in the literature concerning drug-cyclodextrin complexation (32, 33). It can also be observed that the greatest value of Kc was obtained by complexation with β-CDs (natural and modified) compared to αCDs and γCDs, indicating that the bonding strength between camptothecin and this type of CDs is more important, meaning that their size cavities are more adequate to load CPT. Similar equilibrium constants were obtained by Kang et al. (15) and Saetern et al. (8).

From these results, HP-β-CD and PM-β-CD, the two best CPT solubilizers, were selected for further experiments, considering β-CD as reference.

Selection of adequate polymer and concentration

The percentages of CPT released from each SD according to mass percentage and type of PEG are presented in Figure 6. Kinetic release of CPT from each SDs was realized in triplicate.

Improvement of the drug dissolution in all cases is probably attributed to the hydrophilic nature of the polymers (26, 31), with wettability increasing (34) and amorphization of the drug by the carriers in solid dispersions (35). It clearly appeared that PEG 6000 was the best polymer improving CPT dissolution. Moreover, 90% of PEG (w/w) seems to be the most efficient with the less variation on the basis of relative standard deviation (36). For this reason, PEG 6000 at 90% (w/w) was selected for further experiments.

Characterization of inclusion complexes and solid dispersions

FT-IR analysis

Figures 7 and 8 represent the FT-IR spectra of CPT binary and ternary systems.

FT-IR spectroscopy analysis showed that there were weak interactions between the drug and the carrier used in complexation or solid dispersion. This is clearly observed with contracting and disappearance of the drug peaks around: 1750 cm^{-1} corresponding to C=O stretching vibration of lactone ring, 1655 cm^{-1} corresponding to C=O stretching vibration of ketone groups and 1490 cm^{-1} corresponding to vibrations of phenyl rings (37–40). The physical mixture FT-IR spectra showed simultaneously the presence of characteristic peaks of CPT, PEG 6000 and CDs, suggesting that there is no interaction. On the basis of these results, it can be retained that whole drug or at least some of drug groups are incorporated into cyclodextrin cavities and also suggest that there is intermolecular interaction between CPT and PEG molecules.

Differential scanning calorimetry (DSC)

Differential scanning calorimetry thermograms of pure drug and carriers, CPT binary systems and

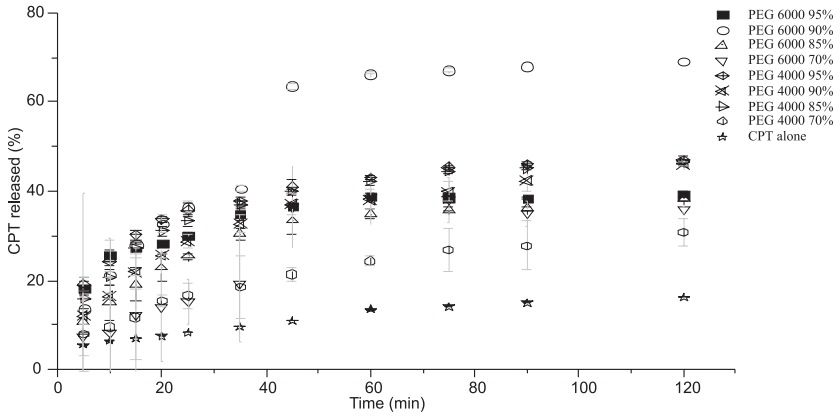

Figure 6. Camptothecin kinetic release from SDs at 5/95, 10/90, 15/85, 30/70 (w/w) percentages

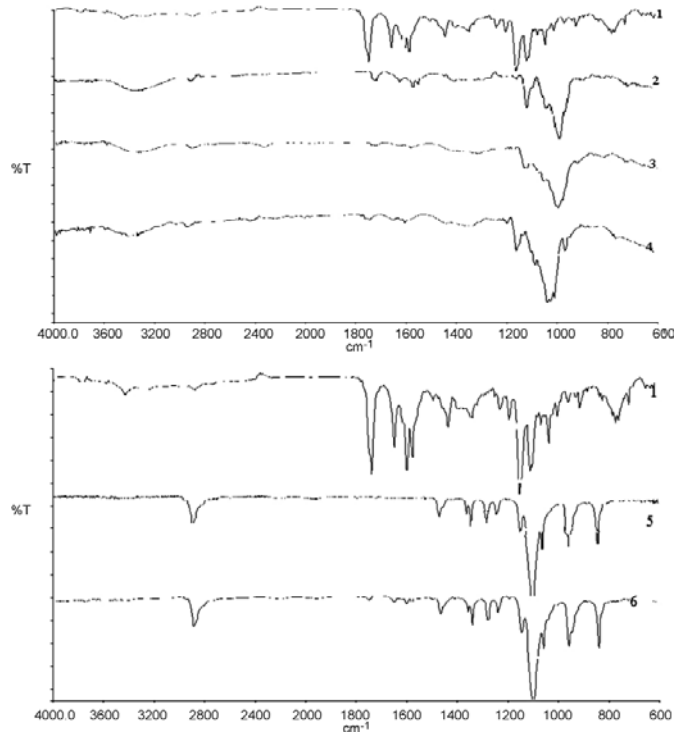

Figure 7. FT-IR spectra of: 1) CPT, 2) (CPT/β-CD) complex, 3) (CPT/HPβ-CD) complex, (CPT/PMβ-CD) complex, 5) PEG 6000 and 6) (CPT/PEG 6000) SD

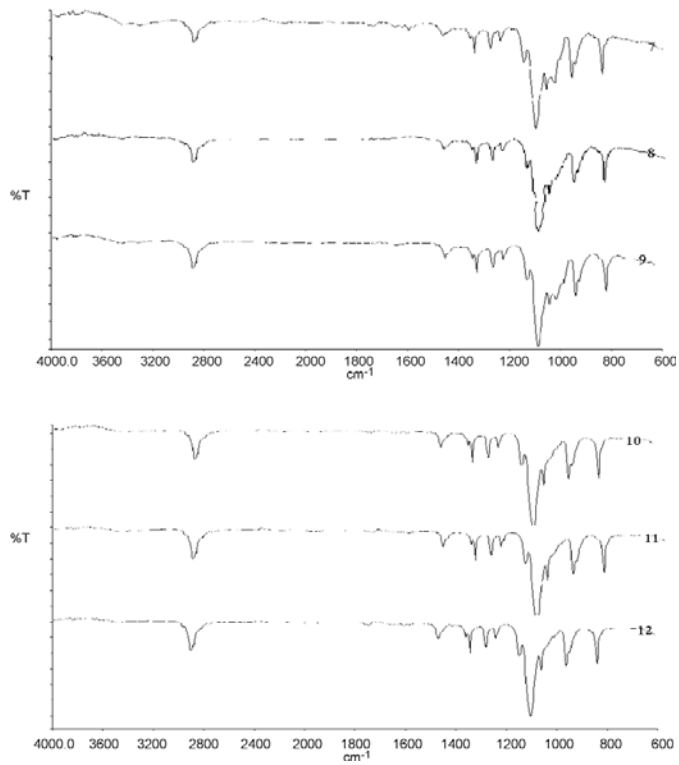

Figure 8. FT-IR spectra of: (7 SD1 ((CPT/β-CD)/PEG 6000), (8 SD2 ((CPT/HPβ-CD)/PEG 6000), (9 SD3 ((CPT/PMβ-CD)/PEG 6000), (10 PM1 ((CPT/β-CD)/PEG 6000), (11 PM2 ((CPT/HPβ-CD)/PEG 6000) and (12 PM3 ((CPT/β-–CD)/PEG 6000)

CPT ternary systems are shown in Figures 9–11. Melting endotherms of CPT which are around 265 and 273°C (indicating crystalline nature of the drug (41)) disappeared totally in thermograms corresponding to CPT/CDs complexes, CPT/PEG 6000 SD (SDo) and CPT complexes/PEG 6000. In contrast, they remained present in PM thermograms. This may indicate inclusion of CPT within the CD cavity replacing water. In case of SDs, only endothermic peak of PEG at 67°C is observed, the disappearance of CPT melting endotherms indicated the absence of crystalline drug replaced by its amorphous form (28,

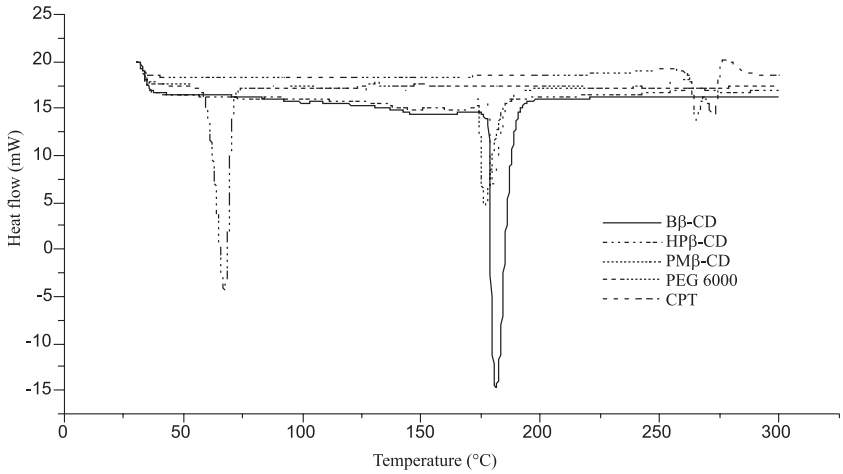

Figure 9. Differential scanning calorimetry thermograms of pure materials

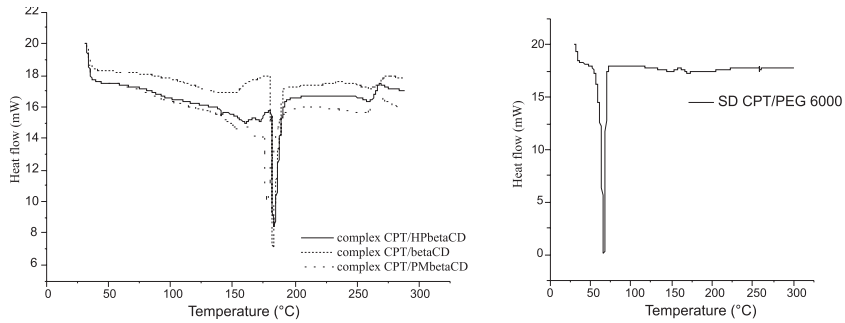

Figure 10. Differential scanning calorimetry thermograms of CPT binary systems, CPT complexes (left) and SD (right)

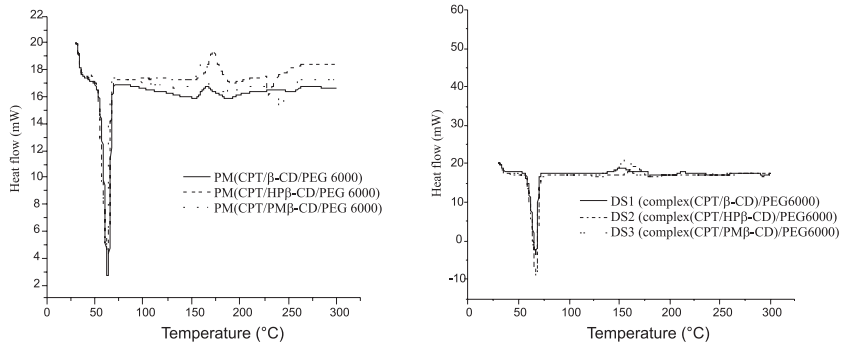

Figure 11. Differential scanning calorimetry thermograms of CPT ternary systems and corresponding physical mixtures

Table 2. Weight loss percentages of CDs, complexes and SDs calculated from dehydration step of TGA.

Analyzed products	Dehydration step		
	Temperature range (°C)		Weight loss (%)
βCD	30	119	12.60
HP-βCD	30	108	5.35
PMβCD	30	108	5.42
CPT/ βCD complex (IC 1)	30	102	4.98
CPT/ HP-βCD complex (IC 2)	30	102	4.50
CPT/ PM-βCD complex (IC 3)	30	102	4.80
SD (CPT/ βCD complex) / PEG (SD1)	30	107	1.57
SD (CPT/ HP-βCD complex)/PEG (SD2)	30	107	0.99
SD (CPT/ PM-βCD complex)/PEG (SD3)	30	107	1.40

Table 3. Drug release kinetic data obtained from fitting the drug release experimental data to different mathematical model of drug release.

	IC 1	IC 2	IC 3	SD 1	SD 2	SD 3	SDo
Zero order model							
Ko	0.0023	0.0028	0.0027	0.0022	0.0024	0.0027	0.0051
R^2	0.83	0.65	0.90	0.63	0.55	0.80	0.79
First order model							
K_1	0.0035	0.0044	0.0070	0.0080	0.0090	0.0100	0.0100
R^2	0.87	0.69	0.96	0.75	0.67	0.90	0.83
Higuchi model							
K_H	0.031	0.041	0.037	0.033	0.037	0.039	0.072
R^2	0.94	0.80	0.98	0.79	0.71	0.91	0.90
Korsmeyer-Peppas model							
K_P	0.20	0.17	0.40	0.54	0.53	0.50	0.14
R^2	0.90	0.75	0.96	0.78	0.69	0.89	0.87
n	0.09	0.12	0.06	0.047	0.052	0.055	0.18

n = diffusional exponent; K = kinetic constant; R^2 = correlation coefficient.

40–42). The DSC thermograms indicated the formation of inclusion complex between CDs and CPT and also indicated a significant dispersion of CPT or its corresponding complexes in PEG 6000. Similar findings have been reported for CPT complexation with HP-β-CD and β-CD by Cirpanli et al. (32).

Thermogravimetric analysis (TGA)

It is reported that through the formation of host-guest inclusion complexes, the thermal stabilities of CDs and guests should be affected (43). The thermogravimetic graphs of pure drug, carriers, complexes and SDs are shown in Figures 12 and 13. Drug showed 84% weight loss, started around 145°C and stabilized around 639°C. This is probably related to the decomposition of CPT structure induced by the transition from solid to liquid phase. PEG 6000 showed 98% weight loss, from 166 to 478°C indicating the decomposition of the polymer. Cyclodextrins presented three stages of weight loss (Fig. 12), where less than 120°C the lost weight indicates the loss of water molecules included in CDs cavities. The weight loss percentages of each CD are presented in Table 2.

Previous studies have reported the presence of water molecules, depending on the relative humidity in CDs (44, 45). Consequently, weight loss in the range 270–500°C was related to CD structure decomposition due to the transition from solid to liquid phase (44). Relatively slow weight decrease

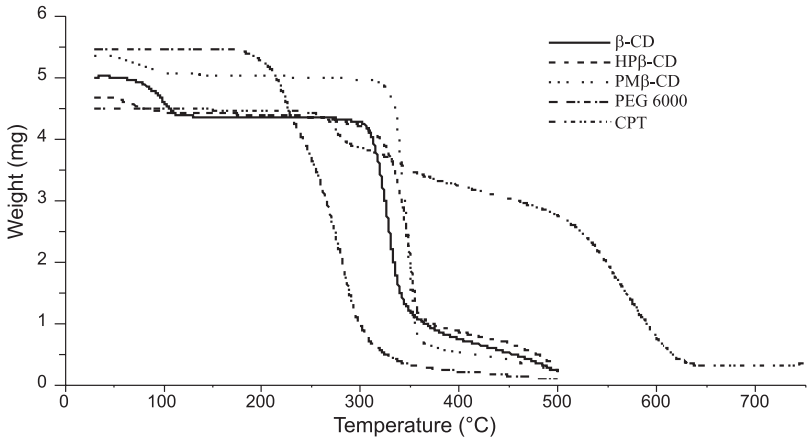

Figure 12. Thermogravimetic graphs of pure CPT and carriers.

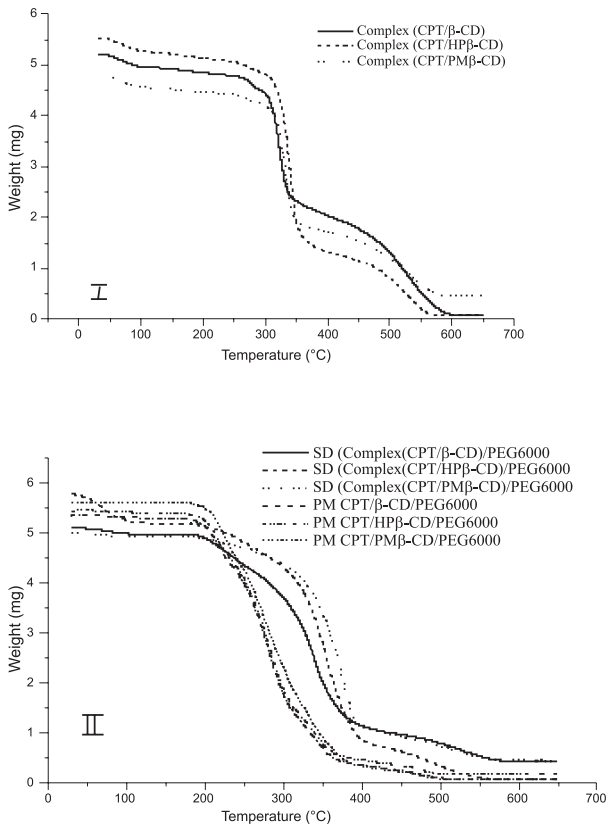

Figure 13. Thermogravimetic graphs of CPT/CDs complexes (I) and thermogravimetic graphs of (CPT/CDs complexes)/PEG 600 SDs (II)

around 500°C indicated the thermal degradation of "chars", the residues formed during the second stage of CDs decomposition (44).

For the both binary and ternary systems, the thermogram patterns were different from the pure materials and since the ranges of degradation of both drug and carrier change, this difference indicates the occurrence of interactions between the drug and carriers and in consequence, the formation of new systems. It is also found in the present study that the dehydration patterns of binary and ternary systems (Table 2) were different from the thermal behavior of pure CDs. The percentages of water evaporation decreased when complexes are formed indicating

substitution of water molecules by CPT, and this decrease was more important when complexes are dispersed in PEG 6000. This fact could be explained by the substitution of water molecules by CPT in one hand, and by the solid dispersion method itself that eliminates most water molecules, in other hand. Surprisingly, the thermogram patterns of PM (CPT/CDs/PEG 6000), did not show any evaporation of water molecules, probably in relation to mass dominance of PEG 6000 and to none homogenous systems. This can also be supported by the similarity of thermogram patterns of SDs and pure PEG 6000.

X-ray powder diffraction (XRPD)

XRPD of raw materials, binary and ternary systems are shown in Figures 14 and 15. The CPT diffractogram revealed a crystalline compound, showing a very strong diffraction peaks at 2θ of 6°, 9°, 11°, 12°, 17.6° and 25°. Nevertheless, the XRD pattern of CPT complexes and solid dispersions (binary and ternary systems) showed that some characteristic peaks of pure CPT were absent and others appeared with a markedly reduced intensity. This suggests the formation of CD inclusion complexes by intermolecular interaction as reported earlier (46, 47). This also demonstrates that the CPT crystalline state dispersed in PEG 6000 had changed to an amorphous form, with improvement of drug dissolution as demonstrated below. This phenomenon had been reported for etoricoxib when it is dispersed in PEG (34).

Dissolution studies

The *in vitro* dissolution profiles of CPT, various ICs, SDo (binary systems) and various SDs of inclusion complexes in PEG 6000 (ternary systems) are shown in Figure 16.

Binary system

The fastest dissolution rate and the most important dissolved percentage of camptothecin were obtained with CPT/ PM-βCD complex, 76% of the drug was dissolved within 120 min. It was also

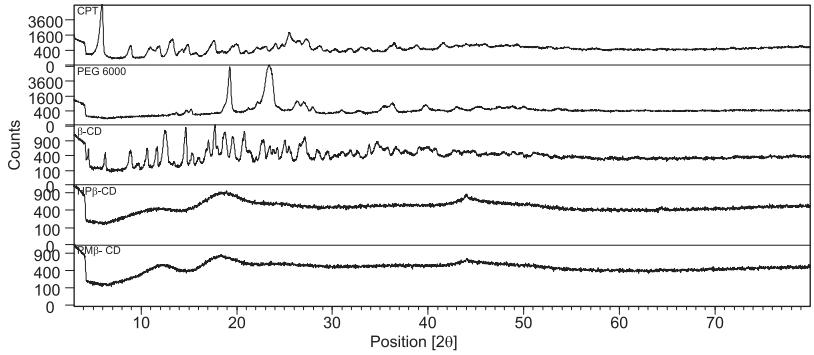

Figure 14. XRPD diffraction of raw materials

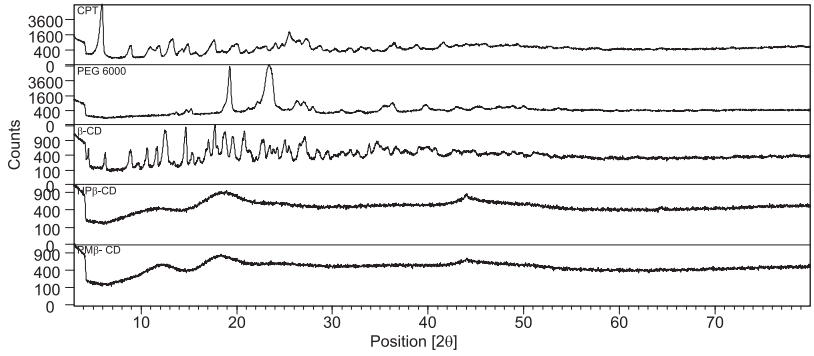

Figure 15. XRPD diffraction of CPT binary and ternary systems

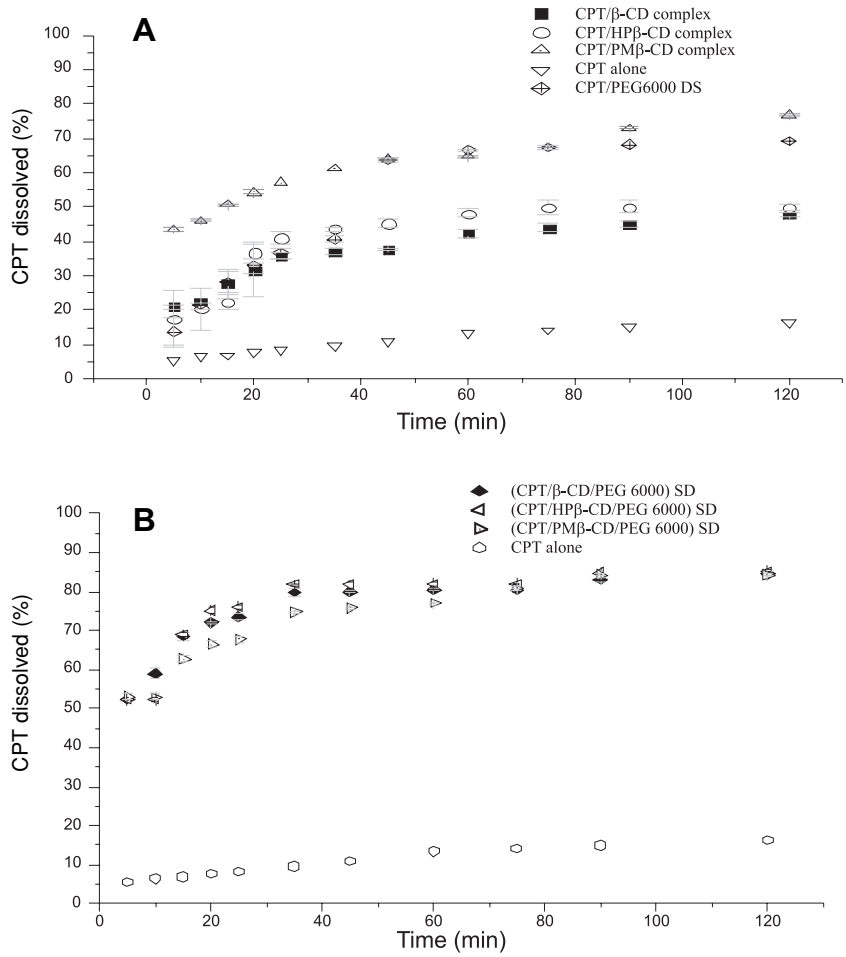

Figure 16. *In vitro* percentage of CPT released from binary (**A**) and ternary (**B**) systems in 0.1 M HCl. Triplicates for each sample except CPT (n = 3)

observed that solid dispersion was more effective in enhancing CPT dissolution (70%) than HP-βCD and βCD complexes. This is probably related to drug crystallinity decrease and the wettability improvement related to PEG 6000 as demonstrated for progesterone and indomethacin SDs (42, 48). The present results demonstrated that solid dispersion of CPT in PEG 6000 is a valuable concurrent to CPT / CDs complexes.

Ternary system

All SDs samples showed dissolution improvement when compared to CPT alone. This is mainly attributed in one part to the formation of inclusion complex, in the second part to wettability increasing by PEG 6000 and to the amorphous state of CPT in SDs preparation. It is also observed that all solid dispersions revealed more CPT dissolution when compared to their respective complexes. This is probably due to the effect of PEG 6000 and to the solid dispersion preparation. (35, 42, 48). Surprisingly, in all SDs preparations, whatever the IC used, 85% of dissolved CPT is reached, a recommendable value for tablet drug release (36), which indicates that there is a synergic effect between CDs and PEG 6000 without regards to the CD substitutions.

In order to establish the mathematical modeling of CPT release, the experimental data were fitted to kinetic models: zero order, first order, Higuchi, and Korsmeyer-Peppas models (49–51).The values for the diffusional exponent (n), correlation coefficient (R^2) and release rate coefficient (k) obtained are summarized in Table 3. The best correlation coefficients (R^2) were obtained with Higuchi model, as it was reported by Costa in his review (52). Higuchi describes drug release as a diffusion

process based in the Fick's law, square root time dependent. When modelization was done by Korsmeyer-Peppas model, the value of the exponent n for all formulations was below 0.43, which was further indicative of the drug releases following Fickian diffusion control mechanism (50, 53).

CONCLUSION

The purpose of the present paper was the improvement of camptothecin solubility and its dissolution rate. These aims were achieved either by forming CPT/CDs complexes, by solid dispersion of 10% of camptothecin in PEG 6000 (w/w) or by formation of ternary systems (CPT/CDs/PEG 6000). HPβ-CD and PMβ-CD appeared to be the most efficient in solubilizing CPT, these two CDs in addition to β-CD enhanced the velocity and the percentage of dissolved CPT, achieving 76% after 120 min, particularly when using PMβ-CD. Moreover, CPT release from solid dispersion (CPT/PEG 6000, 10/90% (w/w)) reached a significant percentage (70%). However, the ternary systems, whatever the CPT complex used, appeared to be the most potent in enhancing the dissolution percentages and velocities. Physicochemical characterization (FT-IR, DSC, TGA and XRPD) demonstrated that camptothecin is incorporated into cyclodextrin cavity, replacing the water molecules. CPT 10% (w/w) or its complexes equivalent are well dispersed in PEG 6000, with appearance of amorphous state of the drug.

The synergic effect of complexation by cyclodextrins and solid dispersion in PEG 6000 conduced to a CPT release following Fickian diffusion reaching 85% in a gastric medium. This main result, offers promising perspectives of new CPT formulation tablets combining the use of non expensive, non toxic and commonly solubilizing carriers: β-CD and PEG 6000.

REFERENCES

1. Paranjpe P.V., Chen Y., Kholodovych V., Welsh W., Stein S., Sinko P.J.: J. Control. Release 100, 275 (2004).
2. Hsiang Y.H., Hertzberg R., Hecht S., Liu L.F.: J. Biol. Chem. 260, 14873 (1985).
3. Li Q.Y., Zu Y.G., Shi R.Z., Yao L.P.: Curr. Med. Chem. 13, 2021 (2006).
4. Thiele C., Auerbach D., Jung G., Wenz G.: J. Incl. Phenom. Macrocycl. Chem. 69,303 (2011).
5. Xie C., Li X., Luo X., Yang Y., Cui W., Zou J., Zhou S.: Int. J. Pharm. 391, 55 (2010).
6. Berrada M., Serreqi A., Dabbarh F., Owusu A., Gupta A., Lehnert S.: Biomaterials 26, 2115 (2005).
7. Lorence A., Nessler C.L.: Phytochemistry 65, 2735 (2004).
8. Saetern A.M., Nguyen N.B., Bauer-Brandl A., Brandl M.: Int. J. Pharm. 284,61 (2004).
9. Cheng J., Khin K.T., Jensen G.S., Liu A., Davis M.E.: Bioconjugate Chem. 14,1007 (2003).
10. Watanabe M., Kawano K., Yokoyama M., Opanasopit P., Okano T., Maitani Y.: Int. J. Pharm. 308,183 (2006).
11. Greenwald R.B., Pendri A., Conover C.D., Lee C., Choe Y.H., Gilbert C., Martinez A. et al.: Bioorg. Med. Chem. 6, 551 (1998).
12. Cýrpanli Y., Allard E., Passirani C., Bilensoy E., Lemaire L., Calyþ S., Benoit J.P.: Int. J. Pharm. 403, 201 (2011).
13. Aiping Z., Jianhong L., Wenhui Y.: Carbohyd. Polym. 63, 89 (2006).
14. Jiang Y., Sha X., Zhang W., Fang X.: Int. J. Pharm. 397, 116 (2010).
15. Kang J., Kumar V., Yang D., Chowdhury P.R., Hohl R.J.: Eur. J. Pharm. Sci. 15, 163 (2002).
16. Cirpanli Y., Bilensoy E., Dogan A.L., Calis S.: J. Control. Release 148, e21 (2010).
17. Bhaskara-Amrit U.R., Agrawal P.B., Warmoeskerken M.C.G.: Autex Res. J. 11, 94 (2011).
18. Katagery A., Sheikh M.: Int. Res. J. Pharm. 3, 52 (2012).
19. Lala R., Thorat A., Gargote C.: IJRAP 2, 1520 (2011).
20. Loftsson T., Duchene D.: Int. J. Pharm.. 329, 1 (2007).
21. Chadha R., Kapoor V., Thankur D., Kaur R., Arora P., Jain D.V.S.: J. Sci. Ind. Res. India 67, 185 (2008).
22. Cheng T.L., Chuang K.H., Chen B.M., Roffler S.R.: Bioconjugate Chem. 23, 881 (2011).
23. Banerjee S.S., Aher N., Patil R., Khandare J.: J. Drug Deliv. 10, 1155 (2012).
24. Dodziuk H.: Cyclodextrins and Their Complexes, p. 2, Wiley-VCH, Weinheim 2006.
25. Li W., Zhan P., De Clercq E., Lou H., Liu X.: Prog. Polym. Sci. 38, 421 (2012).
26. Brewster M.E., Loftsson T.: Adv. Drug Deliv. Rev. 59, 645 (2007).
27. Giri T.K., Kumar K., Alexander A., Ajazuddin, Badwaik H., Tripathi D.K.: Bulletin of Faculty of Pharmacy, Cairo University 50, 147 (2012).
28. Hasnain M.S., Nayak A.K.: Chemistry: Bulgarian Journal of Science Education 21, 118 (2012).

29. Dash S., Murthy P.N., Nath L., Chowdhury P.: Acta Pol. Pharm. Drug Res. 67, 217 (2010).
30. Barzegar-Jalali M., Adibkia K., Valizadeh H., Shadbad M.R., Nokhodchi A., Omidi Y., Mohammadi G. et al.: J. Pharm. Pharm. Sci. 11, 167 (2008).
31. Foulon C., Tedou J., Lamerie T.Q., Vaccher C., Bonte J.P., Goossens J.F.: Tetrahedron Asymmetry 20, 2482 (2009).
32. Cirpanli Y., Bilensoy E., Lale Doğan A., Caliş S.: Eur. J. Pharm. Biopharm. 73, 82 (2009).
33. Bricout H., Hapiot F., Ponchel A., Tilloy S., Monflier E.: Sustainability 1, 924 (2009).
34. Suhagia B.N., Patel H.M., Shah S.A., Rathod I., Parmar V.K. Acta Pharm. 56, 285 (2006).
35. Almeida H.M., Cabral Marques H.M.: J. Incl. Phenom. Macrocycl. Chem. 70, 397(2011).
36. The United States Pharmacopeia 30, NF 25, p. 1010, Rockville, Maryland 2007.
37. Swaminathan S., Pastero L., Serpe L., Trotta F., Vavia P., Aquilano D., Trotta M. et al.: Eur. J. Pharm. Biopharm. 74, 193 (2010).
38. Dong L., Li Y., Hou W.G., Liu S.J.: J. Solid State Chem. 183, 1811 (2010).
39. Guijin L., Hongdi W., Yanbin J.: Ind. Eng. Chem. Res. 52, 15049 (2013).
40. Bai L., Song L.X., Wang M., Zhu L.H.: Chinese J. Chem. Phys. 23, 117 (2010).
41. Thakral N.K., Ray A.R., Bar-Shalom D., Eriksson A.H., Majumdar D.K.: AAPS PharmSciTech 13, 59 (2012).
42. Wulff M., Aldén M.: Eur. J. Pharm. Sci. 8, 269 (1999).
43. Dutet J., Lahiani-Skiba M., Didier L., Jezequel S., Bounoure F., Barbot C., Arnaud P., Skiba M.: J. Incl. Phenom. Macrocycl. Chem. 10, 203 (2007).
44. Zafid M.S., Afidah A.R., Abdullah J.M., Shariza A.R.: Biomed. Res. India 23, 513 (2012).
45. Moriwaki C., Costa G.L., Ferracini C.N., Moraes F.F., Zanin G.M., Pineda E.A.G., Matioli G.: Braz. J. Chem. Eng. 25, 225 (2008).
46. Shaikh J., Ankola D.D., Beniwal V., Singh D., Kumar M.N.: Eur. J. Pharm. Sci. 37, 223 (2009).
47. Yallapu M.M., Jaggi M., Chauhan S.C.: Colloids Surface B 79, 113 (2010).
48. Lahiani-Skiba M., Barbot C., Bounoure F., Joudieh S., Skiba M.: Drug Dev. Ind. Pharm. 32, 1043 (2006).
49. Takahashi A.I., Veiga F.J.B, Ferraz H.G.: Int. J. Pharm. Sci. Rev. Res. 12, 1 (2012).
50. Muthu M.S., Singh S.: Curr. Drug Deliv. 6, 62 (2009).
51. Dredan J., Antal I., Racz I.: Int. J. Pharm. 145, 61 (1996).
52. Costa P., Sousa Lobo J.M. : Eur. J. Pharm. Sci. 13, 123 (2001).
53. Zhang X., Zhang X., Wu Z., Gao X., Cheng C., Wang Z., Li C.: Acta Biomater. 7, 585 (2011).

Received: 10. 12. 2013